Contact Representations of Graphs in 3D

Md. Jawaherul Alam[1], William Evans[2], Stephen G. Kobourov[1], Sergey Pupyrev[1], Jackson Toeniskoetter[1], and Torsten Ueckerdt[3]

[1]Department of Computer Science, University of Arizona, USA
[2]Department of Computer Science, University of British Columbia, Canada
[3]Department of Mathematics, Karlsruhe Institute of Technology, Germany

Abstract

We study contact representations of graphs in which vertices are represented by axis-aligned polyhedra in 3D and edges are realized by non-zero area common boundaries between corresponding polyhedra. We show that for every 3-connected planar graph, there exists a simultaneous representation of the graph and its dual with 3D boxes. We give a linear-time algorithm for constructing such a representation. This result extends the existing primal-dual contact representations of planar graphs in 2D using circles and triangles. While contact graphs in 2D directly correspond to planar graphs, we next study representations of non-planar graphs in 3D. In particular we consider representations of optimal 1-planar graphs. A graph is 1-planar if there exists a drawing in the plane where each edge is crossed at most once, and an optimal n-vertex 1-planar graph has the maximum $(4n-8)$ number of edges. We describe a linear-time algorithm for representing optimal 1-planar graphs without separating 4-cycles with 3D boxes. However, not every optimal 1-planar graph admits a representation with boxes. Hence, we consider contact representations with the next simplest axis-aligned 3D object, L-shaped polyhedra. We provide a quadratic-time algorithm for representing optimal 1-planar graph with L-shaped polyhedra.

1 Introduction

Graphs are often used to capture relationships between objects, and graph embedding techniques allow us to visualize such relationships via traditional node-links diagrams. There are compelling theoretical and practical reasons to study *contact representations* of graphs, where vertices are geometric objects and edges correspond to pairs of objects touching in some specified fashion. In practice, 2D contact representations with rectangles, circles, and polygons of low complexity are intuitive, as they provide the viewer with the familiar metaphor of geographical maps. Such representations are preferred in some contexts over the standard node-link representations for displaying relational information [13, 25]. Contact representations of graphs have practical applications in data visualization [42], cartography [37], geography [45], sociology [29], very-large-scale integration circuit design [46], and floor-planning [34].

A large body of work considers representing graphs as contacts of simple curves or polygons in 2D. Graphs that can be represented in this way are planar. In fact, Koebe's 1936 theorem established that *all* planar graphs can be represented by touching disks [32]. Any planar graph also has a contact representation with triangles [20, 26]. Partial planar 3-trees and some series-parallel graphs admit a representation with homothetic triangles [3]. Curve contacts [27], line-segment contacts [18, 33], and L-shape contacts [14, 31] have also been used. In particular, it is known that all planar bipartite graphs can be represented by axis-aligned segment contacts [16, 19, 39]. Furthermore, any planar graph has a representation with T-shapes [20]. Despite our best efforts, however, many graphs remain stubbornly non-planar and, for these, such contact representations in 2D are impossible. Hence, a

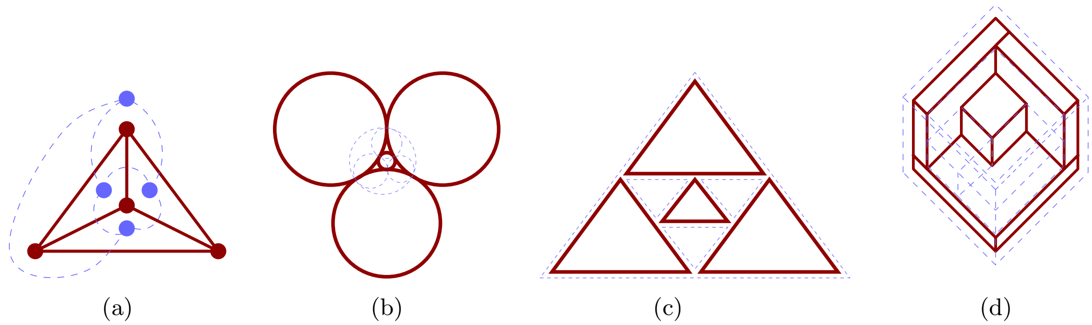

Figure 1: (a) A planar graph K_4 and its dual; primal-dual contact representations of the graph with (b) circles and (c) triangles. (d) The primal-dual box-contact representation of K_4 with dual vertices shown dashed. The outer box (shell) contains all other boxes.

natural generalization is representing vertices with 3D-polyhedra, such as cubes and tetrahedra, and edges with shared boundaries. While such contact representations allow us to visualize non-planar graphs, there is much less known about contact representations in 3D than in 2D. Contact graphs using 3D objects have been studied for complete graphs and complete bipartite graphs using spheres [8, 28] and cylinders [7].

As a first step towards representing non-planar graphs, we consider *primal-dual* contact representations, in which a plane graph (a planar graph with a fixed planar embedding) and its dual are represented simultaneously. More formally, in such a representation vertices and faces are represented by some geometric objects so that:

(i) the objects for the vertices are interior-disjoint and induce a contact representation for the primal graph;

(ii) the objects for the faces are interior-disjoint except for the object for the outer face, which contains all the objects for the internal faces, and together they induce a contact representation of the dual graph;

(iii) the objects for a vertex v and a face f of the primal graph intersect if and only if v and f are incident.

Primal-dual representations of planar graphs have been studied in 2D. Specifically, every 3-connected plane graph has a primal-dual representation with circles [1] and triangles [26]; see Fig. 1(a)–(c). Our first result in this paper is an analogous primal-dual representation using axis-aligned 3D boxes. While it is known that every planar graph has a contact representation with 3D boxes [44, 23, 11], Theorem 1 strengthens these results; see Fig. 1d.

Theorem 1. *Every 3-connected planar graph $G = (V, E)$ admits a proper primal-dual box-contact representation in 3D and it can be computed in $\mathcal{O}(|V|)$ time.*

We would like to mention two differences with the existing primal-dual representations [1, 26]. First, both of these existing constructions induce *non-proper* (point) contacts, while our contacts are always *proper*, that is, have non-zero areas. Second, for a given 3-connected plane graph, it is not always possible to find a primal-dual representation with circles by a polynomial-time algorithm [5], although it can be constructed numerically by polynomial-time iterative schemes [15, 35]. There is also no known polynomial-time algorithm that computes a primal-dual representation with triangles for a given 3-connected plane graph. Our representation, in contrast, can be found in linear time and can be realized on the $n \times n \times n$ grid, where n is the number of vertices of the graph.

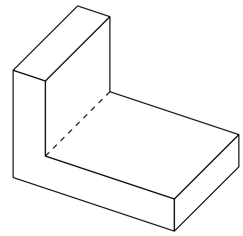

Figure 2: An L-shaped polyhedron.

We prove Theorem 1 with two different constructive algorithms. The first one uses the notions of Schnyder woods and orthogonal surfaces, as defined in [24]. Although it is known that every 3-connected planar graph induces an orthogonal surface, we show how to construct a new contact representation with interior-disjoint boxes from the orthogonal surface. Since the orthogonal surfaces for a 3-connected planar graph and its dual coincide topologically, the primal and the dual box-contact representations can be fit together to realize the desired contacts. The alternative algorithm builds a box-contact representation for a maximal planar graph using the notion of a canonical order of planar graph [21]. Both construction ideas are inspired by recent box-contact representation algorithms for maximal planar graphs [11]; however, we generalize the algorithms to accommodate 3-connected planar graphs and show that the primal and dual representations can be combined together. Our methods rely on a correspondence between Schnyder woods and generalized canonical orders for 3-connected planar graphs. Although the correspondence has been claimed earlier in [4], the earlier proof appears to be incomplete. As another contribution of the paper, we provide a complete proof of the claim in Section 2.2.

Theorem 1 immediately gives box-contact representations for a special class of non-planar graphs that are formed by the union of a planar graph and its dual. The graphs are called *prime* and are defined as follows. A simple graph $G = (V, E)$ is said to be 1-*planar* if it can be drawn on the plane so that each of its edges crosses at most one other edge. This class of graphs was first considered by Ringel [38] in the context of simultaneously coloring a planar graph and its dual. A 1-planar graph has at most $4|V| - 8$ edges [22, 36] and it is *optimal* if it has exactly $4|V| - 8$ edges, that is, it is the densest 1-planar graph on the vertex set [9, 10]. An optimal 1-planar graph is called *prime* if it has no separating 4-cycles, that is, cycles of length 4 whose removal disconnects the graph. These optimal 1-planar graphs are exactly the ones that are 5-connected and the ones that can be obtained as the union of a 3-connected simple plane graph, its dual and its vertex-face-incidence graph [41]. Note that in our primal-dual representation not all boxes are interior-disjoint, as one of the boxes contains all other boxes. We call this special box the *shell* and such a representation a *shelled* box-contact representation. Here all the vertices are represented by 3D boxes, except for one vertex, which is represented by a shell, and the interiors of all the boxes and the exterior of the shell are disjoint. Note that a similar shell is also required in the circle-contact and triangle-contact representations; see Fig. 1. The following is a direct corollary of Theorem 1.

Corollary 2. *Every prime* 1*-planar graph* $G = (V, E)$ *admits a shelled box-contact representation in 3D and it can be computed in* $\mathcal{O}(|V|)$ *time.*

One may wonder whether every 1-planar graph admits a box-contact representation in 3D, but it is easy to see that there are 1-planar graphs, even as simple as K_5, that do not admit a box-contact representation. Furthermore, there exist optimal 1-planar graphs (which contain separating 4-cycles) that have neither a box-contact representation nor a shelled box-contact representation.

Therefore, we consider representations with the next simplest axis-aligned object in 3D, an L-shaped polyhedron or simply an $\mathcal{L}$, which is an axis-aligned box minus the intersection of two axis-aligned half-spaces; see Fig. 2. Such an object can also be considered as the union of two boxes in 3D. In the paper, we provide a quadratic-time algorithm for representing every optimal 1-planar graph

with $\mathcal{L}$'s.

Theorem 3. *Every optimal* 1*-planar graph* $G = (V, E)$ *has a proper* $\mathcal{L}$*-contact representation in 3D and it can be computed in* $\mathcal{O}(|V|^2)$ *time.*

Our algorithm is similar to a recursive procedure used for constructing box-contact representations of planar graphs in [23, 44]. The basic idea is to find separating 4-cycles and represent the inner and the outer parts of the graph induced by the cycles separately. Then these parts are combined together to produce the final representation. Since the separating 4-cycles can be nested inside each other, the running time of our algorithm is dominated by the finding of separating 4-cycles and the nested structure among them. Unlike the early algorithms for box-contact representations of planar graphs [23, 44], our algorithms produce proper contacts between the 3D objects (boxes and $\mathcal{L}$'s).

2 Preliminaries

Here we introduce the tools needed to prove our results. In Section 2.1 we define the known concepts of an *ordered path partition* and a *Schnyder wood*. In Section 2.2 we describe new results about the relationship between these two structures for 3-connected plane graphs. Section 2.4 reviews the concept of an *orthogonal surface*.

2.1 Ordered Path Partitions, Canonical Orders and Schnyder Woods

The concepts of a Schnyder wood and a canonical order were initially introduced for maximal plane graphs [21, 40]; later they were generalized to 3-connected plane graphs [30, 24]. Although the concepts are proved to be equivalent for maximal plane graphs [17], they are no longer equivalent after the generalization. Thus Badent et al. [4] generalized the notion of a canonical order to an *ordered path partition* for a 3-connected plane graph in an attempt to make it equivalent to a Schnyder wood.

Let G be a 3-connected plane graph with a specified pair of vertices $\{v_1, v_2\}$ and a third vertex $v_3 \notin \{v_1, v_2\}$, such that v_1, v_2, v_3 are all on the outer face in that counterclockwise order. Add the edge (v_1, v_2) to the outerface of G (if it does not already contain it) and call the augmented graph G'. Let $\Pi = (V_1, V_2, \ldots, V_L)$ be a partition of the vertices of G. Then Π is an *ordered path partition* of G if the following conditions hold:

(1) V_1 contains the vertices on the clockwise path from v_1 to v_2 on the outer cycle; $V_L = \{v_3\}$;

(2) for $1 \leq k \leq L$, the subgraph G_k of G' induced by the vertices in $V_1 \cup \ldots \cup V_k$ is 2-connected and internally 3-connected (that is, removing two internal vertices of G_k does not disconnect it); and the outer cycle C_k of G_k contains the edge (v_1, v_2);

(3) for $2 \leq k \leq L$, each vertex on C_{k-1} has at most one neighbor on V_k.

The pair of vertices (v_1, v_2) forms the *base-pair* for Π and v_3 is called the *head vertex* of Π. For an ordered path partition $\Pi = (V_1, V_2, \ldots, V_L)$ of G, we say that a vertex v of G has *level* k if $v \in V_k$. The *predecessors* of v are all the vertices with equal or smaller levels and the *successors* of v are all vertices with equal or larger levels; see Fig. 3a.

The definition of a *canonical order* is similar to that for an ordered path partition, but for Condition (3), which is replaced by the following more restricted Condition (3'):

(3') for $2 \leq k \leq L$, V_k is a (left-to-right) path $\{v_a, v_{a+1}, \ldots v_b\}$, which is a subpath of $C_k - (v_1, v_2)$, and each v_i with $i \in \{a, \ldots, b\}$ has at least one neighbor in $G - G_k$. If $a < b$ then each of v_a and v_b has one neighbor on C_{k-1} and these are the only neighbors of V_k in G_{k-1}. If $a = b$ then $v_a = v_b$ may have multiple neighbors on C_{k-1}.

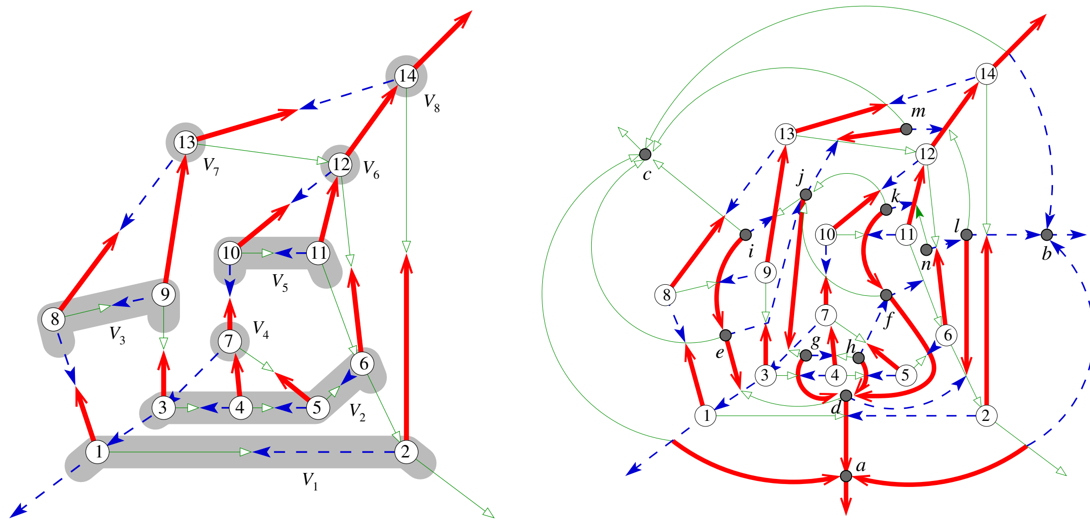

(a) (b)

Figure 3: (a) An ordered path partition and its corresponding Schnyder wood for a 3-connected graph G. (b) The Schnyder woods for the primal and the dual of G. The thick solid red, dotted blue and thin solid green edges represent the three trees in the Schnyder wood.

Thus a canonical order is a special ordered path partition and the definition of the *base-pair*, *head vertex*, *predecessors* and *successors* follow from that in an ordered path partition.

A Schnyder wood is defined as follows. Let v_1, v_2, v_3 be three specified vertices in that counterclockwise order on the outer face of G. For $i = 1, 2, 3$, add a half-edge from v_i reaching into the outer face. Then a *Schnyder wood* is an orientation and coloring of all the edges of G (including the added half edges) with the colors $1, 2, 3$ satisfying the following conditions:

(1) every edge e is oriented in either one (*uni-directional edge*) or two opposite directions (*bi-directional edge*). The edges are colored and if e is bi-directional, then the two directions have distinct colors;

(2) the half-edge at v_i is directed outwards and colored i;

(3) each vertex v has out-degree exactly one in each color, and the counterclockwise order of edges incident to v is: outgoing in color 1, incoming in color 2, outgoing in color 3, incoming in color 1, outgoing in color 2, incoming in color 3;

(4) there is no interior face whose boundary is a directed cycle in one color.

These conditions imply that for $i = 1, 2, 3$, the edges with color i induce a tree $\mathcal{T}_i$ rooted at v_i, where all edges of $\mathcal{T}_i$ are directed towards the root. We denote the Schnyder wood by $(\mathcal{T}_1.\mathcal{T}_2, \mathcal{T}_3)$. Every 3-connected plane graph G has a Schnyder wood [24, 6]. From a Schnyder wood of G, one can construct a *dual Schnyder wood* (the Schnyder wood for the dual of G). Consider the dual graph G^* of G in which the vertex for the outer face of G has been split into three vertices forming a triangle. These three vertices represent the three regions between pairs of half edges from the outer vertices of G. Then a Schnyder wood for G^* is formed by orienting and coloring the edges so that between an edge e in G and its dual e^* in G^*, all three colors $1, 2, 3$ are used. In particular, if e is uni-directional in color i, $i = 1, 2, 3$, then e^* is bi-directional in colors $i - 1$, $i + 1$ and vice versa; see Fig. 3b.

2.2 Correspondence

Let G be a 3-connected plane graph with a specified base-pair (v_1, v_2) and a specified head vertex v_3 such that v_1, v_2, v_3 are in that counterclockwise order on the outer face. It is known that an ordered

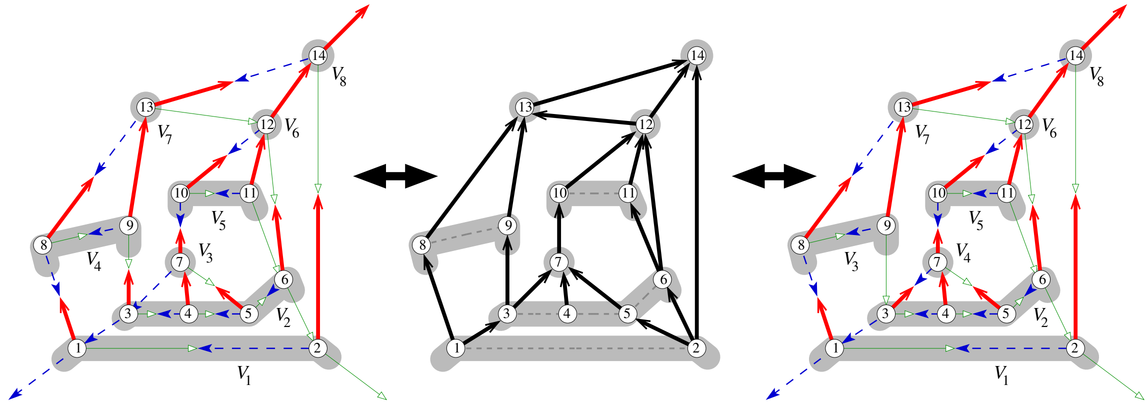

Figure 4: Two ordered path partition with their compatible Schnyder woods (left and right) that gives the same acyclic graph D_i after reversing the direction of the edges in two trees and grouping all cyclic maximal paths. Thus starting with either Schnyder wood can give either ordered path partition by the algorithm in [4].

path partition of G defines a Schnyder wood on G, where the three outgoing edges for each vertex are to its (1) leftmost predecessor, (2) rightmost predecessor, and (3) highest-level successor [24, 6]. We call an ordered path partition and the corresponding Schnyder wood computed this way to be *compatible* with each other. Badent et al. [4] claim that the converse can also be done, that is, given a Schnyder wood on G, one can compute an ordered path partition, compatible with the Schnyder wood (and hence, there is a one-to-one correspondence between the concepts). However, it turns out that the algorithm in [4] for converting a Schnyder wood to a compatible ordered path partition is incomplete[1], that is, the computed ordered path partition is not always compatible with the Schnyder wood; see Fig. 4 for an example. Here we provide a correction for the algorithm.

Let $(\mathcal{T}_1, \mathcal{T}_2, \mathcal{T}_3)$ be a Schnyder wood of G. From here on whenever we talk about Schnyder woods, we consider a circular order for the indices $i = 1, 2, 3$ so that $(i-1)$ and $(i+1)$ are well defined when $i \in \{1, 2, 3\}$. By [24] there is no cycle of G that is directed in $\mathcal{T}_{i-1}^{-1} \cup \mathcal{T}_{i+1}^{-1} \cup \mathcal{T}_i$, where $\mathcal{T}_i^{-1}$, $i = 1, 2, 3$, denotes the reversed edges of $\mathcal{T}_i$. Since there are some bi-directional edges in G colored with $i+1$ and $i-1$ (which we call *cyclic*), $\mathcal{T}_{i-1}^{-1} \cup \mathcal{T}_{i+1}^{-1} \cup \mathcal{T}_i$ induces some directed cycles of length 2. We can form a directed acyclic graph D_i by *grouping* each maximal path in $\mathcal{T}_{i-1}^{-1} \cup \mathcal{T}_{i+1}^{-1} \cup \mathcal{T}_i$ with cyclic bi-colored edges (call such a path a *cyclic maximal path*) into a single vertex. Here the maximal paths P_i with cyclic bi-colored edges are the vertices of D_i, and for two such paths P_i and P_j, there is a directed edge from P_i to P_j in D_i whenever there is a directed (not cyclic) edge (u, v) in $\mathcal{T}_{i-1}^{-1} \cup \mathcal{T}_{i+1}^{-1} \cup \mathcal{T}_i$ for some $u \in P_i$ and $v \in P_j$. Badent et al. [4] showed that D_i is acyclic and they suggest to obtain an ordered path partition by taking a topological order of D_i. However, the resulting ordered path partition is not necessarily compatible with $(\mathcal{T}_1, \mathcal{T}_2, \mathcal{T}_3)$ and Fig. 4 shows an example. Instead, before grouping the cyclic maximal paths, we augment the graph $\mathcal{T}_{i-1}^{-1} \cup \mathcal{T}_{i+1}^{-1} \cup \mathcal{T}_i$ with the following directed edges. For each vertex v of G, we add a directed edge from each child of v in $\mathcal{T}_{i-1}$ and $\mathcal{T}_{i+1}$ to the parent of v in $\mathcal{T}_i$. The augmented graph remains acyclic and it is consistent with the partial order defined by D_i (we call this the *partial order defined by* $(\mathcal{T}_{i-1}^{-1} \cup \mathcal{T}_{i+1}^{-1} \cup \mathcal{T}_i)$). A topological order of the augmented graph (after grouping all cyclic maximal paths) induces a compatible ordered path partition.

Lemma 4. *Let $(\mathcal{T}_1, \mathcal{T}_2, \mathcal{T}_3)$ be a Schnyder wood of a 3-connected plane graph G with three specified vertices v_1, v_2, v_3 in that counterclockwise order on the outer face. Then for $i = 1, 2, 3$ one can compute in linear time an ordered path partition Π_i compatible with $(\mathcal{T}_1, \mathcal{T}_2, \mathcal{T}_3)$ such that Π_i has (v_{i-1}, v_{i+1}) as the base pair and v_i as the head. The ordered path partition is consistent with the partial order*

[1] Confirmed by a personal communication with the authors of [4].

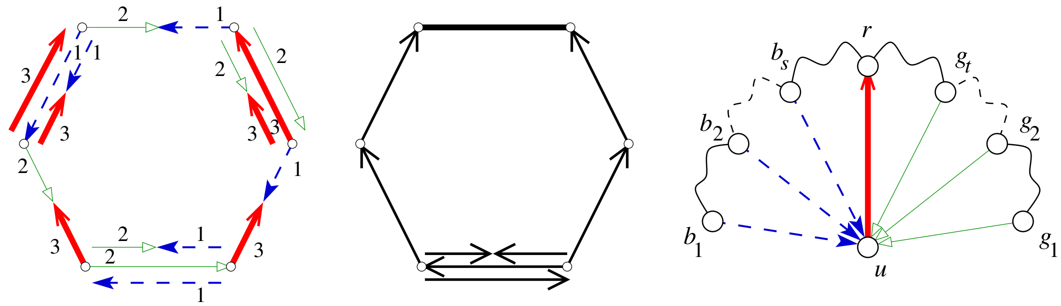

(a) (b) (c)

Figure 5: (a) Coloring and orientation of the edges around a generic face in to a Schnyder wood $(\mathcal{T}_1, \mathcal{T}_2, \mathcal{T}_3)$, (b) orientation of the edges in $D_3 = (\mathcal{T}_2^{-1} \cup \mathcal{T}_1^{-1} \cup \mathcal{T}_3) \setminus \mathcal{T}_{2,1}$, (c) directed paths in $\mathcal{T}_2^{-1} \cup \mathcal{T}_1^{-1} \cup \mathcal{T}_3$ from children of a vertex u in $\mathcal{T}_1$ and $\mathcal{T}_2$ to the parent in $\mathcal{T}_3$.

defined by $(\mathcal{T}_{i-1}^{-1} \cup \mathcal{T}_{i+1}^{-1} \cup \mathcal{T}_i)$.

Proof. Consider the directed acyclic graph D_i by grouping each cyclic maximal path of $(\mathcal{T}_{i-1}^{-1} \cup \mathcal{T}_{i+1}^{-1} \cup \mathcal{T}_i)$ into a single vertex. D_i is acyclic since by [24], no cycle in G is directed in $\mathcal{T}_{i-1}^{-1} \cup \mathcal{T}_{i+1}^{-1} \cup \mathcal{T}_i$. Furthermore each vertex in D_i has at least two predecessors, one in $\mathcal{T}_{i-1}^{-1}$ and one in $\mathcal{T}_{i+1}^{-1}$. Therefore one can compute an ordered path partition of G by taking a topological ordering Π of D_i and for each vertex u of G assigning u label k where $u \in U$ and k is the rank of U in Π; see [4] for details. However the ordered path partition obtained by this procedure might not be compatible with $(\mathcal{T}_1, \mathcal{T}_2, \mathcal{T}_3)$; in particular for a vertex u of G, its parent in T_i might not be its highest-level successor; see Fig. 4.

In order to ensure compatibility between the Schnyder wood and the obtained ordered path partition, we further augment D_i by adding some extra edges. In particular, for each vertex u of G, if v is its parent in $\mathcal{T}_i$ and w is it child in either $\mathcal{T}_{i-1}$ or $\mathcal{T}_{i+1}$, then we add a directed edge (V, W) in D_i^* where V, W are cyclic maximal paths in D_i and $v \in V$, $w \in W$. Call the augmented directed graph H_i. We now show that with the addition of the extra edges the directed graph H_i remains acyclic. We prove this claim only for H_3; for H_1 and H_2 the proofs are analogous.

Consider an arbitrary face f of G. By [24], the edges on the boundary of f can be partitioned into at most six consecutive sets in clockwise order around f (see Fig. 5(a)):

(i) one edge from the set clockwise in color 1, counterclockwise in color 2, bi-colored with a clockwise 1 and counterclockwise 2

(ii) zero or more edges bi-colored in counterclockwise 2 and clockwise 3

(iii) one edge from the set clockwise in color 3, counterclockwise in color 1, bi-colored with a clockwise 2 and counterclockwise 1

(iv) zero or more edges bi-colored in counterclockwise 1 and clockwise 2

(v) one edge from the set clockwise in color 2, counterclockwise in color 3, bi-colored with a clockwise 2 and counterclockwise 3

(vi) zero or more edges bi-colored in counterclockwise 3 and clockwise 1

Fig. 5(b) shows the direction of the edges of f in D_3. Now consider a vertex u of G. Let r be its parent in $\mathcal{T}_3$, b_1, …, b_s its children in $\mathcal{T}_1$ in clockwise order around u, and g_1, …, g_t its children in $\mathcal{T}_2$ in counterclockwise order around u. Thus $L = b_1, \ldots, b_s, r, g_t, \ldots, g_1$ appears consecutively around u in that clockwise order. Let P_i^b, $i = 1, \ldots, s$ be the paths from b_i to its next vertex in L that forms the face of G containing these two vertices and u; see Fig. 5(c). Similarly let P_i^g, $i = 1, \ldots, t$ be the

paths from g_i to its previous vertex in L that forms the face of G containing these two vertices and u. From Fig. 5(b) one can see that all the paths P_i^b and P_i^g are directed towards r (possibly with some bi-directional edges) in D_3. This imply that for each vertex b_i, $i = 1 \ldots, s$ (resp. g_i, $i = 1, \ldots, t$), there is a directed path (possibly with some bi-directional edges) from b_i (resp. g_i) to r. Thus adding an edge from any b_i or g_i to r does not create any cycle in D_3 since otherwise replacing the edge with the directed path induces a directed cycle in $\mathcal{T}_2^{-1} \cup \mathcal{T}_1^{-1} \cup \mathcal{T}_3$, a contradiction. Since the addition of the extra edges does not make any cycle in D_3, the graph H_3 remains acyclic.

Once we add the extra edges, we can compute an ordered path partition consistent with D_i, by taking a topological ordering of H_i and for each vertex u of G, assigning k as its label where $u \in U$ for some cyclic maximal path U in D_i and k is the rank of U in the topological ordering of H_i. This ordered path partition is compatible with $(\mathcal{T}_1, \mathcal{T}_2, \mathcal{T}_3)$ since for each vertex u, the parents of u in $\mathcal{T}_{i-1}$ and in $\mathcal{T}_{i+1}$ are the leftmost and rightmost predecessors (due to the embedding) and the parent in $\mathcal{T}_i$ is the highest-level successor (due to the addition of the extra edges).

The time complexity of the above algorithm is linear. Computing the directed graph D_i, $i = 1, 2, 3$ can be done by traversing the edges of G. Addition of the extra edges takes $\sum_{v \in V(G)} deg(v) = 2|E(G)| = \mathcal{O}(n)$ time also. Finally the topological ordering can be done by a linear-time Depth-first traversal on the graph H_i, which also has a linear size. $\square$

Fig. 6 illustrates the three ordered path partitions computed from a Schnyder wood of a 3-connected plane graph using the algorithm described above.

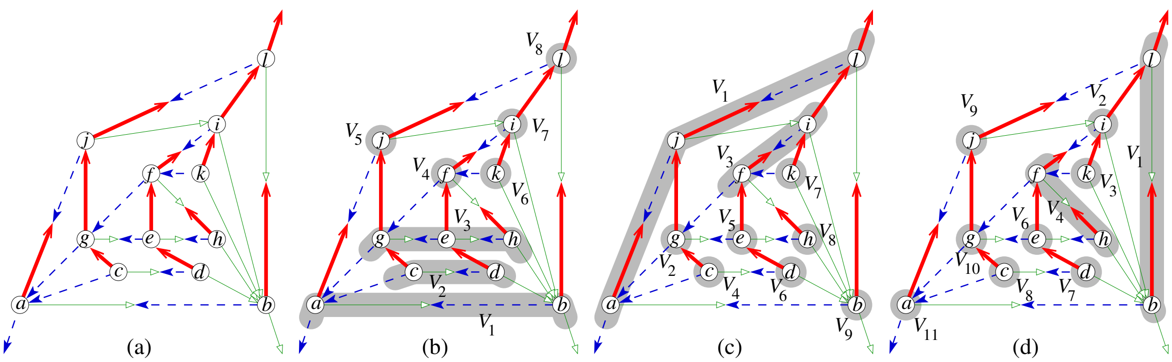

Figure 6: (a) A Schnyder wood $(\mathcal{T}_1, \mathcal{T}_2, \mathcal{T}_3)$ in a 3-connected plane graph G, which is not compatible with any canonical order, (b)–(d) the three compatible ordered path partition computed from $(\mathcal{T}_1, \mathcal{T}_2, \mathcal{T}_3)$ using the algorithm described in the proof of Lemma 4.

2.3 Elementary Canonical Orders and Elementary Schnyder Woods

Here we introduce the concepts of *elementary* canonical orders and *elementary* Schnyder woods, which we use in the subsequent section for an alternate proof for Theorem 1.

A canonical order $\Pi = (V_1, V_2, \ldots, V_L)$ for a 3-connected plane graph G is *elementary* if (i) $|V_1| = 2$ (or equivalently the base-pair (v_1, v_2) induces an edge on the outer cycle). Kant showed that any 3-connected plane graph G, with an edge (v_1, v_2) and a third vertex v_3, both on the outer cycle, has an elementary canonical order for the base pair (v_1, v_2) and head v_3 and such an elementary canonical order for G can be computed in linear time [30].

Not all Schnyder woods are compatible with canonical orders; Fig. 6(a) shows an example of a Schnyder wood that is not compatible with any canonical order. Let $\Pi = (V_1, V_2, \ldots, V_L)$ be a canonical order in a 3-connected plane graph G with a specified base-pair (v_1, v_2) and a specified head vertex v_3 such that v_1, v_2, v_3 are in that counterclockwise order on the outer face. Let $(\mathcal{T}_1, \mathcal{T}_2, \mathcal{T}_3)$ be the Schnyder wood compatible with Π. Then by the definition of compatible Schnyder wood, it follows

that for every maximal path $P = \{u_1, u_2, \ldots u_t\}$ in $(\mathcal{T}_1, \mathcal{T}_2, \mathcal{T}_3)$ with each edge (u_j, u_{j+1}) bi-colored in color 1 and 2 for $1 \leq j < t$, there is no child of the vertices $u_2, \ldots, u_{t-1}$ in $\mathcal{T}_3$, and the only children of u_1 and u_t in $\mathcal{T}_3$ (if any) are respectively the parent of u_1 in $\mathcal{T}_1$ and the parent of u_t in $\mathcal{T}_3$. We call this property for a Schnyder wood $(\mathcal{T}_1, \mathcal{T}_2, \mathcal{T}_3)$ the *canonical property* of the Schnyder wood for color 3. One can define the canonical property of a Schnyder wood analogously for colors 1 and 2. Let $(\mathcal{T}_1, \mathcal{T}_2, \mathcal{T}_3)$ be a Schnyder wood for a 3-connected plane graph G with three specified vertices v_1, v_2, v_3 in that counterclockwise order on the outer face. Then $(\mathcal{T}_1, \mathcal{T}_2, \mathcal{T}_3)$ is *elementary* for the color i, $i = 1, 2, 3$, if (i) (v_{i-1}, v_{i+1}) is an edge on the outer cycle, and (ii) the canonical property holds for color i in $(\mathcal{T}_1, \mathcal{T}_2, \mathcal{T}_3)$.

Lemma 5. *Let G be a 3-connected plane graph with three specified vertices v_1, v_2, v_3 in the counterclockwise order on the outer face of G. Let Π_i be an ordered path partition of G with a specified base-pair (v_{i-1}, v_{i+1}) and a specified head vertex v_i for $i = 1, 2, 3$ and let $(\mathcal{T}_1, \mathcal{T}_2, \mathcal{T}_3)$ be the compatible Schnyder wood for Π. Then Π_i is an elementary canonical order if and only if $(\mathcal{T}_1, \mathcal{T}_2, \mathcal{T}_3)$ is an elementary Schnyder wood for color i.*

Proof. The lemma follows from the definitions of elementary canonical order and elementary Schnyder wood and from the observation that the maximal paths in $(\mathcal{T}_1, \mathcal{T}_2, \mathcal{T}_3)$ bi-colored with colors $i - 1$ and $i + 1$ are in one-to-one correspondence with the paths of G with the same level in Π_i, $i = 1, 2, 3$. □

We end this section with the following lemma.

Lemma 6. *If a Schnyder wood $(\mathcal{T}_1, \mathcal{T}_2, \mathcal{T}_3)$ for a 3-connected plane graph G is elementary for color i, $i = 1, 2, 3$, then its dual Schnyder wood is also elementary for color i in the dual graph of G.*

Proof. We prove this lemma only for color 3, since the proof for color 1 or 2 is similar. By definition the outer cycle for the dual graph of G for constructing the dual Schnyder wood is a triangle; hence the base-pair for the dual Schnyder wood are adjacent. Hence for the dual Schnyder wood to be elementary it is sufficient that for each $P = \{u_1, u_2, \ldots u_t\}$ with each edge (u_j, u_{j+1}) bi-colored in 1 and 2 for $1 \leq j < t$, (i) there is no child of the vertices $u_2, \ldots, u_{t-1}$ in $\mathcal{T}_3$, and (ii) the only child of u_1 and u_t in $\mathcal{T}_3$ (if any) are respectively the parent of u_1 in $\mathcal{T}_1$ and the parent of u_t in $\mathcal{T}_2$. However, the way we define the color and orientation of the edges in the dual, failure to satisfy Condition (i) for some path in the dual Schnyder wood implies that Condition (ii) does not hold for some path in the primal Schnyder wood and vice versa; see Fig. 7. Therefore if the primal Schnyder wood is elementary in color 3, so is the dual Schnyder wood. □

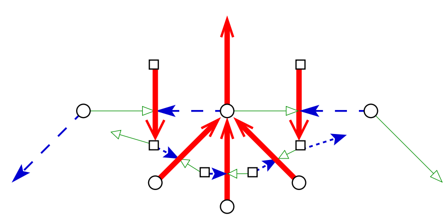

Figure 7: Illustration for the proof of Lemma 6.

2.4 Orthogonal Surfaces

Here we briefly review the notion of orthogonal surfaces, which we use in the proof for Theorem 1; see [24] for more details. A point p in $\mathbb{R}^3$ *dominates* another point q if the coordinate of p is greater than or equal to q in each dimension; p and q are *incomparable* if neither of p nor q dominates the other. Given a set M of incomparable points, an *orthogonal surface* defined by M is the geometric

boundary of the set of points that dominate at least one point of M. For two points p and q, their *join*, $p \vee q$ is obtained by taking the maximum coordinate of p, q in each dimension separately. The *minimums* (*maximums*) of an orthogonal surface S are the points of S that dominate (are dominated by) no other point of S. An orthogonal surface S is *rigid* if for each pair of points p and q of M such that $p \vee q$ is on S, $p \vee q$ does not dominate any point other than p and q. An orthogonal surface is *axial* if it has exactly three unbounded orthogonal arcs. Rigid axial orthogonal surfaces are known to be in one-to-one correspondence with Schnyder woods of 3-connected plane graphs [24] and the rigid axial orthogonal surfaces S and S^* corresponding to a Schnyder wood and its dual coincide with each other, where the maximums of S are the minimums of S^* and vice versa.

3 Primal-Dual Representations of 3-Connected Planar Graphs

Here we prove Theorem 1.

Theorem 1. *Every* 3*-connected planar graph* $G = (V, E)$ *admits a proper primal-dual box-contact representation in 3D and it can be computed in* $\mathcal{O}(|V|)$ *time.*

Specifically, we describe two different linear-time algorithms that compute a box-contact representation for the primal graph and the dual graph separately and then fits them together to obtain the desired result. In the first algorithm we compute the coordinates of the boxes based on a Schnyder wood, in the second, we compute them based on an elementary canonical order. Both these algorithms guarantee that the boundary for the primal (dual) representation induces an *orthogonal surface* compatible with the dual (primal) Schnyder wood. Since the orthogonal surfaces for a Schnyder wood and its dual coincide topologically, we can fit together the primal and the dual box-contact representation to obtain a desired representation.

To avoid confusion, we denote a connected region in a plane embedding of a graph by a *face*, and a side of a 3D shape by a *facet*. For a 3D box R, call the facet with highest (lowest) x-coordinate as the x^+-facet (x^--facet) of R. The y^+-facet, y^--facet, z^+-facet and z^--facets of R are defined similarly. For convenience, we sometimes denote the x^+-, x^-, y^+-, y^-, z^+- and z^--facets of R as the *right*, *left*, *front*, *back*, *top* and *bottom* facets of R, respectively.

3.1 Construction Based on Schnyder Woods

We first construct a contact representation Γ of the primal graph G with boxes in 3D. Let v_1, v_2 and v_3 be three vertices on the outer face of G in counterclockwise order. We compute a Schnyder wood $(\mathcal{T}_1, \mathcal{T}_2, \mathcal{T}_3)$ such that for $i = 1, 2, 3$, $\mathcal{T}_i$ is rooted at v_i. By Lemma 4, for $i = 1, 2, 3$, one can compute a compatible ordered path partition with the base-pair (v_{i-1}, v_{i+1}) and head v_i, which is consistent with the partial order defined by $(\mathcal{T}_{i-1}^{-1} \cup \mathcal{T}_{i+1}^{-1} \cup \mathcal{T}_i)$. Denote by $<_X$, $<_Y$ and $<_Z$ the three ordered path partitions compatible with $(\mathcal{T}_1, \mathcal{T}_2, \mathcal{T}_3)$, that are consistent with D_1, D_2, and D_3, respectively. We use these three ordered path partitions to define our box-contact representation for G.

For a vertex u, let $x_M(u)$, $y_M(u)$, and $z_M(u)$ be the levels of u in the ordered path partitions $<_X$, $<_Y$, and $<_Z$, respectively. Define $x_m(u) = x_M(b)$, $y_m(u) = y_M(g)$ and $z_m(u) = z_M(r)$, where b, g and r are the parents of u in $\mathcal{T}_1$, $\mathcal{T}_2$ and $\mathcal{T}_3$, respectively, whenever these parents are defined. For each of the three special vertices v_i, $i = 1, 2, 3$, the parent is not defined in $\mathcal{T}_i$. We assign $x_m(v_1) = 0$, $y_m(v_2) = 0$ and $z_m(v_3) = 0$.

Now for each vertex u of G, define a box $R(u)$ representing u as the region $[x_M(u), x_m(u)] \times [y_M(u), y_m(u)] \times [z_M(u), z_m(u)]$. Denote by R the set of all boxes $R(u)$ for the vertices u of G. We show in Lemma 7 that R yields a box-contact representation for G. Furthermore, for each edge (u, v) of G, if (u, v) is uni-colored then $R(u)$ and $R(v)$ make a proper contact. Otherwise, assume w.l.o.g. that (u, v) is bi-colored with colors 1 (oriented from u to v) and 2 (oriented from v to u). Then $x_m(u) = x_M(v)$, $y_M(u) = y_m(v)$, $z_M(u) = z_M(v)$; $R(u)$ and $R(v)$ make a non-proper contact along the line-segment $\{x_m(u)\} \times \{y_m(v)\} \times [z_M(u), z^*]$, where $z^* = \min\{z_m(u), z_m(v)\}$. However since v is

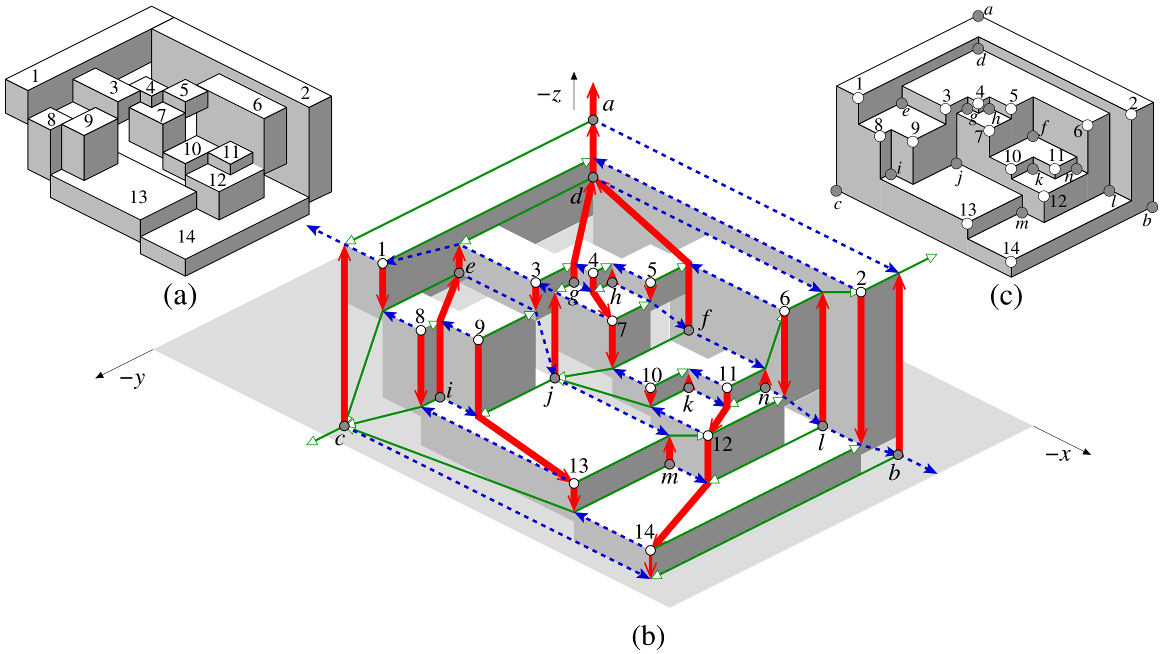

Figure 8: Box-contact representation (a) for the graph in Fig. 3 with its primal-dual Schnyder wood (b) and the associated orthogonal surface (c). The thick solid red, dotted blue and thin solid green edges represent the three trees in the Schnyder wood.

the only parent of u in $\mathcal{T}_1$ and u is the only parent of v in $\mathcal{T}_2$, by Lemma 7, the x^+-facet of $R(u)$ and the y^+-facet of $R(v)$ do not make a proper contact with any box. Hence either extending $R(u)$ in the positive x-direction or extending $R(v)$ in positive y-direction by some small amount $0 < \epsilon < 1$ makes the contact between $R(u)$ and $R(v)$ proper without creating any overlap or unnecessary contacts between the boxes. We thus obtain a proper box-contact representation Γ for the primal graph G.

Now we describe how to construct the box-contact representation for the dual of G. Consider the orthogonal surface induced by Γ. Each vertex v of G corresponds to the $x^-y^-z^-$-corner p of the box for v. The three outgoing edges of v in the Schnyder wood can be drawn on the surface from p in the directions x^+, y^+, z^+; see Fig. 8. Each face of G corresponds to a reflex corner of the orthogonal surface and there is a similar (opposite) direction for the outgoing edges in the dual Schnyder wood. The topology of this (rigid axial) orthogonal surface is uniquely defined by both the Schnyder wood and its dual [24]. Thus, we construct the contact representation Γ' for the dual of G, then (after possible scaling) the boundary of Γ' exactly matches $B - \Gamma$, where B is the bounding box of Γ. We fit Γ and Γ' together by replacing the three boxes for the three outer vertices of G with a single shell-box, which forms the boundary of the entire representation.

It is easy to see that the above algorithm runs in $\mathcal{O}(|V|)$ time. A Schnyder wood for G and the dual Schnyder wood for the dual of G can be computed in linear time [24]. For both the primal graph and the dual graph, the three ordered path partitions can then be computed in linear time from these Schnyder woods, due to Lemma 4. The coordinates of the boxes are then directly assigned in constant time per vertex. Finally the primal and the dual representation can be combined together by reflecting (and possibly scaling) the dual representation, which can also be done in linear time.

Lemma 7 shows the correctness for the above construction; specifically, it shows that the boxes computed in the construction induce a contact representation for G.

Lemma 7. *The set of all boxes $R(u)$ for the vertices u of G induces a contact representation of G, where for each vertex u, the x^+-, y^+-, z^+-facets of $R(u)$ touch the boxes for the parents of u in $\mathcal{T}_1$, $\mathcal{T}_2$, $\mathcal{T}_3$, respectively, and the x^--, y^--, z^--facets of $R(u)$ touch the boxes for the children of u in $\mathcal{T}_1$, $\mathcal{T}_2$,*

$\mathcal{T}_3$*, respectively. Furthermore for each edge* (u, v) *of* G*, the contact between* $R(u)$ *and* $R(v)$ *is proper if and only if* (u, v) *is uni-colored.*

Proof. We prove the lemma by showing the following two claims: (i) for each edge (u, v) of G, the two boxes $R(u)$ and $R(v)$ make contact in the specified facets, (ii) for any two vertices u and v of G, the two boxes $R(u)$ and $R(v)$ are interior-disjoint.

(i) Take an edge (u, v) of G. If (u, v) is uni-colored in G, assume w.l.o.g. that it has color 3 and is directed from u to v. By construction, $z_m(u) = z_M(v)$. We now show that $x_M(v) < x_M(u) < x_m(v)$ and $y_M(v) < y_M(u) < y_m(v)$, which implies the correct contact between $B(u)$ and $B(v)$. Since (u, v) is in $\mathcal{T}_3$ and the ordered path partitions $<_X$ and $<_Y$ are consistent with $\mathcal{T}_3^{-1}$, $x_M(v) < x_M(u)$ and $y_M(v) < y_M(u)$. To show that $x_M(u) < x_m(v)$, consider the parent b of v in $\mathcal{T}_1$. Then $x_m(v) = x_M(b)$. Furthermore, before computing the topological order to find $<_X$, we added the directed edge (u, b); thus $x_M(u) < x_M(b) = x_m(v)$. The proof that $y_M(u) < y_m(v)$ is symmetric.

If (u, v) is bi-colored with colors, w.l.o.g., 1 (orientated from u to v) and 2 (from v to u), then by construction $x_m(u) = x_M(v)$ and $y_M(u) = y_m(v)$. (u, v) is bi-colored in 1, 2, so $z_M(u) = z_M(v)$. Thus, $R(u)$, $R(v)$ make non-proper contact in the correct facets.

(ii) Now we show that for any two vertices u and v of G, $R(u)$ and $R(v)$ are interior-disjoint. By the properties of Schnyder woods, from any vertex u of G, there are three vertex-disjoint paths $P_1(u)$, $P_2(u)$, $P_3(u)$ where $P_i(u)$ is a directed path from u to v_i of edges colored i, $i = 1, 2, 3$. We first claim that for some $i, j \in \{1, 2, 3\}$, $i \neq j$, there is a directed path from u to v, or from v to u in $\mathcal{T}_i \cup \mathcal{T}_j^{-1}$. The claim holds trivially if u is on the directed path $P_i(v)$, or v is on the directed path $P_i(u)$, for some $i \in \{1, 2, 3\}$. Otherwise, assume that v is in the region between $P_2(u)$, and $P_3(u)$. Then the path $P_1(v)$ intersects either $P_2(u)$, and $P_3(u)$ at some vertex w. Assume w.l.o.g. that w is on $P_2(u)$. Then the path P that follows $P_1(v)$ from v to w, and then follows $P_2^{-1}(u)$ from w to u is directed in $\mathcal{T}_2^{-1} \cup \mathcal{T}_1$ (here $P_2^{-1}(u)$ is the path $P_2(u)$ with all the directions reversed). Hence, assume that there is a path from u to v in $\mathcal{T}_1 \cup \mathcal{T}_2^{-1}$. By definition, $x_m(u) \leq x_M(v)$ and thus $R(u)$ and $R(v)$ are interior-disjoint. □

3.2 Construction Based on Elementary Canonical Orders

Here we provide an alternate proof for Theorem 1 by a different construction algorithm than the one in Section 3.1. This algorithm is based on an elementary canonical order and builds a representation iteratively inserting boxes for the vertices in this order. It is similar to the box-contact representation algorithm suggested in [11] for maximal planar graphs. However in addition to generalizing the construction for 3-connected plane graphs, we maintain a stronger invariant on every iteration, in order to accommodate the boxes of the dual graph later on.

We first construct a contact representation Γ of G with boxes. Let v_1, v_2 and v_3 be three vertices on the outer face of G in counterclockwise order such that (v_1, v_2) is an edge on the outer cycle. Compute an elementary canonical order $\Pi = (V_1, \ldots, V_L)$ and the compatible Schnyder wood defined by Π. Let G_k be the graph induced by the vertices in $V_1 \ldots V_k$. We now add boxes representing the vertices in the order defined by Π.

For step 1 of our construction, we add two boxes to represent v_1 and v_2 such that the x^--facet of the box for v_1 touches the x^+-facet of the box for v_2. Their z^--facets lie on the plane $z = 0$ and their z^+-facets on $z = 1$. We maintain the invariant that, at the beginning of step k, the boxes of *active vertices*, that is, the vertices in C_{k-1}, intersect the plane $z = k$ in a *staircase shape*, that is, where the minimum x, y boundary of the intersection is an x, y-monotone axis-aligned polyline where the convex corners are $x^-y^-z^+$-corners of boxes that represent the active vertices consecutively in the order that they appear in the outer face of G_k.

For step $k \geq 2$, we add boxes for the vertices in $V_k = \{v_a, v_{a+1}, \ldots, v_b\}$ with their z^--facets on the plane $z = k - 1$ and their z^+-facets on $z = k$.

If $a = b$, let w_ℓ and w_r be the leftmost and rightmost neighbors of $v_a = v_b$ in C_{k-1}. We create the box for v_a so that its x^+-facet touches box w_ℓ, its y^+-facet touches box w_r, and its z^--facet covers (and touches if $(v_a, w_i) \in E$)) the box for w_i ($\ell < i < r$) (this is possible due to the staircase invariant). Boxes in this last set are now no longer active. By the construction of a compatible Schnyder wood, each edge of v_a added in this step except possibly the edges with w_ℓ and w_r are colored 3 and directed towards v_a. The edge (v_a, w_ℓ) is colored 1 and directed towards w_ℓ, and the edge (v_a, w_r) is colored 2 and directed towards w_r; note that one or both these edges may also be colored 3 and directed towards v_a.

If $a < b$, let w_ℓ and w_r be the neighbors of v_a and v_b, respectively, on C_{k-1}. We create the boxes for $v_a, v_{a+1}, \ldots, v_b$ so that the x-facets or y-facets of the boxes for v_{a+i} and v_{a+i+1} touch. The x^+-facet of box v_a touches box w_ℓ and the y^+-facet of box v_b touches box w_r. By the construction of compatible Schnyder wood, for $1 \leq i < b - a$, the edges (v_{a+i}, v_{a+i+1}) are bi-directional, and the direction from v_{a+i} to v_{a+i+1} is colored 2, while the other direction is colored 1. The edges (v_a, w_ℓ) and (v_b, w_r) are directed and colored as in the case where $a = b$.

In both cases: if (v_a, w_ℓ) is a bi-directional edge (with colors 1 and 3) we align the y^--facets of box v_a and box w_ℓ (note w_ℓ is no longer active); and if (v_b, w_r) is a bi-directional edge (with colors 2 and 3) we align the x^--facets of box v_b and w_r (note w_r is no longer active). We have not yet set the coordinate of the z^+-facet of any of the boxes of V_k. We simply extend the boxes of all active vertices in the $+z$ direction, so that the z^+-facet is in the plane $z = k$.

An illustration of the representation obtained by this algorithm is shown in Fig. 8.

Now we describe how to construct the box-contact representation for the dual of G. Consider the orthogonal surface induced by Γ. Each vertex v of G corresponds to the $x^-y^-z^-$-corner p of the box for v. The three outgoing edges of v in the Schnyder wood can be drawn on the surface from p in the directions x^+, y^+, z^+; see Fig. 8. Each face of G corresponds to a reflex corner of the orthogonal surface and there is a similar (opposite) direction for the outgoing edges in the dual Schnyder wood. The topology of this (rigid axial) orthogonal surface is uniquely defined by both the Schnyder wood and its dual [24]. Thus, we construct the contact representation Γ' for the dual of G using the same algorithm, then (after possible scaling) the boundary of Γ' exactly matches $B - \Gamma$, where B is the bounding box of Γ. We fit Γ and Γ' together by replacing the three boxes for the three outer vertices of G with a single shell-box, which forms the boundary of the entire representation.

The above construction algorithm takes $\mathcal{O}(|V|)$ time. An elementary canonical order of G can be computed in linear time [30] and one can compute a compatible Schnyder wood using the definition in linear time as well. The x, y and z-coordinates of the boxes are computed in constant time for a vertex of a primal graph. Hence, the primal representation of the graph can be found in linear time. Again from the Schnyder wood of G, one can compute a dual Schnyder wood for the dual graph in linear time [24] and by Lemma 4 a compatible elementary canonical order for the dual can also be computed in linear time and the same algorithm can be used to construct the dual representation in linear time. Finally the primal and the dual representation can be combined together by reflecting

The construction for a primal-dual box-contact representation of a 3-connected plane graph G in Theorem 1 has another interpretation. Start with the orthogonal surface S corresponding to both a Schnyder wood of G and its dual. This orthogonal surface S creates two half-spaces on either side of S: extend boxes from S in these half-spaces, so that (i) the boxes are interior-disjoint and (ii) they induce box-contact representations for the primal and dual graphs. However, how to extend the corners and why such a construction yields a proper box-contact representation seems to require the same kinds of arguments that we provided in this section. A "proof from the book" for Theorem 1, using topological properties of the orthogonal surface, is a nice open problem.

4 Representations for Optimal 1-Planar Graphs

In this section we consider contact representation for optimal 1-planar graphs. We first show that there exists optimal 1-planar graphs with no box-contact representation. We thus consider contact

representation for optimal 1-planar graphs with the next simplest axis-aligned 3D object: $\mathcal{L}$'s. We provide a quadratic-time algorithm for representing optimal 1-planar graph with $\mathcal{L}$'s.

4.1 Optimal 1-Planar Graphs with no Box-Contact Representation

Here we prove the following lemma.

Lemma 8.

- *K_5 has no proper box-contact representation in 3D.*
- *There exist optimal 1-planar graphs that have neither box-contact representation nor shelled box-contact representation in 3D.*

Proof. Assume for a contradiction that K_5 has a contact representation Γ with five boxes B_i, $i \in \{1,2,3,4,5\}$. We first show that there is a point o which is common to all five boxes in Γ, that is, $\cap_{i=1}^{5} B_i$ is not empty. Since B_i is an axis-aligned box, one can define B_i as $[x_i, X_i] \times [y_i, Y_i] \times [z_i, Z_i]$ for each $i \in \{1,2,3,4,5\}$. Now for any pair of boxes B_i, B_j, $i, j \in \{1,2,3,4,5\}$, B_i and B_j makes a contact in Γ since Γ represents K_5; hence there is a point (x_{ij}, y_{ij}, z_{ij}) common to B_i, B_j. This can happen only if $x_{ij} \in [x_i, X_i]$, $x_{ij} \in [x_j, X_j]$, $y_{ij} \in [y_i, Y_i]$, $y_{ij} \in [y_j, Y_j]$ and $z_{ij} \in [z_i, Z_i]$, $z_{ij} \in [z_j, Z_j]$. In particular if we look at the projection on the x-axis, $x_i \leq x_{ij} \leq X_i$ and $x_j \leq x_{ij} \leq X_j$; that is, $[x_i, X_i]$ and $[x_j, X_j]$ have a common point x_{ij}. Then by Helly's theorem [2], $[x_i, X_i]$, $i \in \{1,2,3,4,5\}$ have a common point x^*. Similarly all the projections of B_i's on the y-axis (resp. on the z-axis) have a common point y^* (resp. z^*). Then for each box B_i, $(x^*, y^*, z^*) \in B_i$ and therefore (x^*, y^*, z^*) is a common point for all five boxes. Call this point o.

Now consider the eight closed octants with o in the center. Denote the positive and negative x-half-space of o by x_+ and x_-, respectively. Similarly define y_+, y_-, z_+ and z_- to be the positive y-half-space, negative y-half-space, positive z-half-space and negative z-half-space, respectively. Then for $X \in \{x_+, x_-\}$, $Y \in \{y_+, y_-\}$, $Z \in \{z_+, z_-\}$, denote the octant $X \cap Y \cap Z$ by XYZ. Since all five boxes contain o, no octant can contain parts of two or more boxes. Since there are eight octants and five boxes, by pigeonhole principle, there are at least two boxes, each of which are completely contained inside one octant. Assume, w.l.o.g. (after possible renaming), that B_1 and B_2 are these two boxes and they lie on the two octants $x_+y_+z_+$ and $x_+y_+z_-$, respectively. Then for any box to make a proper contact with both B_1 and B_2, it must lie either in both the octants $x_-y_+z_+$, $x_-y_+z_-$, or in both the octants $x_+y_-z_+$, $x_+y_-z_-$. This implies at least one of the three boxes B_3, B_4 and B_5 fails to make a proper contact with at least one of B_1 and B_2. This completes the proof for K_5.

In order to prove the second part of the claim, first note that there exists an almost-optimal 1-planar graph containing K_5 as a subgraph; see Fig. 9. Call this graph G^*. Now consider an optimal 1-planar graph G. Take two faces $f_1 = a_1b_1c_1d_1$ and $f_2 = a_2b_2c_2d_2$ in the quadrangulation of G such

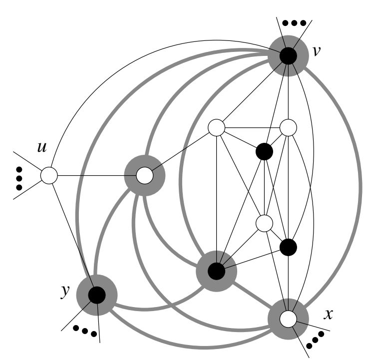

Figure 9: An almost optimal 1-planar graph G^* containing a K_5 (highlighted).

that they do not share vertices. Delete the crossing edges inside the two faces and in each face f_i, $i = 1, 2$, and insert an isomorphic copy of G^*, identifying u, v, x, y with a_i, b_i, c_i, d_i. Let H be the resulting augmented graph. As shown earlier, H has no contact representation with interior-disjoint boxes. Furthermore, H does not admit a shelled box-contact representation, as at least one copy of G^* in H does not contain the vertex represented by the shell. □

4.2 L-Contact Representation of Optimal 1-Planar Graphs

Here we prove Theorems 2 and 3. Throughout, let G be an optimal 1-planar graph with a fixed 1-planar embedding. An edge is *crossing* if it crosses another edge, and *non-crossing* otherwise. A cycle in a connected graph is *separating* if removing it disconnects the graph. We start by listing some well-known properties of optimal 1-planar graphs.

Lemma 9 (Brinkmann *et al.* [12], Suzuki [43])**.**

- *The subgraph of an embedded optimal 1-planar graph G induced by the non-crossing edges is a plane quadrangulation Q with bipartition classes W and B.*
- *The induced subgraphs $G_W = G[W]$ and $G_B = G[B]$ on white and black vertices, respectively, are planar and dual to each other.*
- *The graphs G_B and G_W are 3-connected if and only if Q has no separating 4-cycles.*
- *There exists a simple optimal 1-planar graph with quadrangulation Q if and only if Q is 3-connected.*

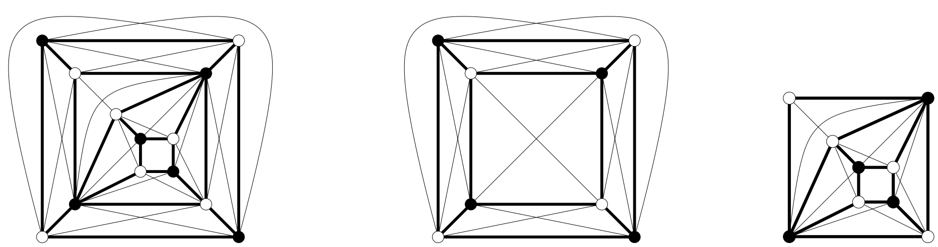

(a) (b) (c)

Figure 10: (a) An embedded optimal 1-planar graph, its quadrangulation Q (bold) and the partition into white and black vertices. (b) The graph G_{out} produced by removing the interior of separating 4-cycle C. (c) The graph $G_{in}(C)$ comprised of the separating 4-cycle and its interior.

Call an optimal 1-planar graph *prime* if its quadrangulation has no separating 4-cycle.

Corollary 2. *Every prime 1-planar graph $G = (V, E)$ admits a shelled box-contact representation in 3D and it can be computed in $\mathcal{O}(|V|)$ time.*

Proof. Let Q be the quadrangulation of G and let B, W be the bipartition classes of Q. By Lemma 9, $G_B = G[B]$ and $G_W = G[W]$ are 3-connected planar and dual to each other. By Theorem 1, a primal-dual box-contact representation Γ of G_B can be computed in linear time. We claim that Γ is a contact representation of G. Indeed, the edges of G are partitioned into G_B, G_W, Q. Each edge in G_B is realized by contact of two "primal" boxes, in G_W by contact of "dual" boxes, and in Q by contact of a primal and a dual box; see Fig. 11. □

Next, assume that G is any (not necessarily prime) optimal 1-planar graph. To find an $\mathcal{L}$-representation for G, we find all separating 4-cycles in G, replace their interiors by a pair of crossing

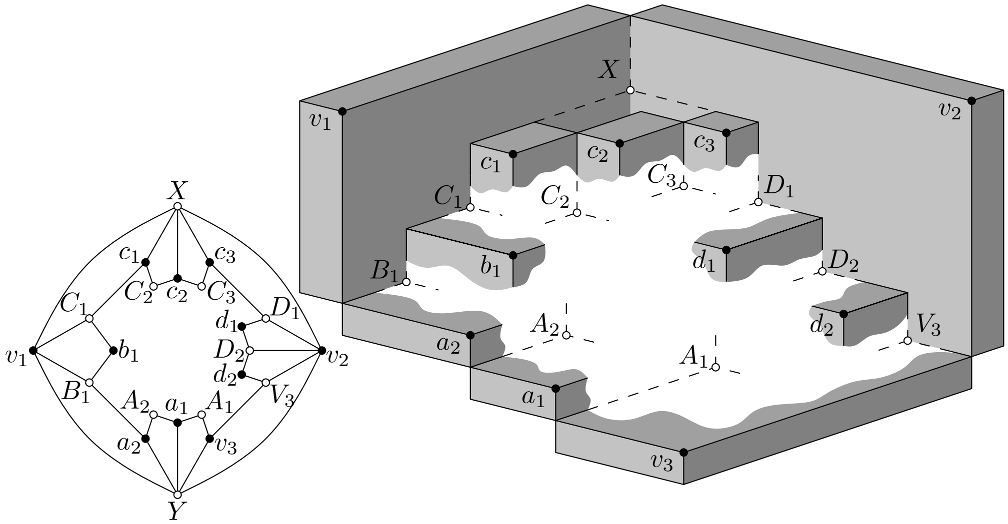

Figure 11: Part of an optimal 1-planar graph and its partial proper box contact representation

edges and construct an $\mathcal{L}$-representation of the obtained smaller 1-planar graph by Corollary 2. We ensure that this $\mathcal{L}$-representation has some "available space" in which we can place the $\mathcal{L}$-representations for the removed subgraph in each separating 4-cycle, which we construct recursively. We remark that similar procedures were used before, e.g., for maximal planar graphs and their separating triangles [23, 44]. A separating 4-cycle is *maximal* if its interior is inclusion-wise maximal among all separating 4-cycles. A 1-planar graph with at least 5 vertices is called *almost-optimal* if its non-crossing edges induce a quadrangulation Q and inside each face of Q, other than the outer face, there is a pair of crossing edges.

Algorithm *L-Contact*(optimal 1-planar graph G)
1. Find all separating 4-cycles in the quadrangulation Q of G
2. **if** some inner vertex w of Q is adjacent to two outer vertices of Q
3. **then** $\mathcal{C}$ = set of the two 4-cycles containing w and 3 outer vertices of Q. **(Case 1)**
   else $\mathcal{C}$ = set of all maximal separating 4-cycles in Q. **(Case 2)**
4. Take the optimal 1-planar (multi)graph G_{out} obtained from G by replacing for each 4-cycle $C \in \mathcal{C}$ all vertices strictly inside C by a pair of crossing edges; see Fig. 10b.
5. Compute an $\mathcal{L}$-representation of G_{out} that has "some space" at each 4-cycle $C \in \mathcal{C}$. In Case 2, this is done from a shelled box-contact representation of G_{out} in Corollary 2.
6. For each $C \in \mathcal{C}$, take the almost-optimal 1-planar subgraph $G_{in}(C)$ of G induced by C and all vertices inside C; see Fig. 10c. Recursively compute an $\mathcal{L}$-representation of $G_{in}(C)$ and insert it into the corresponding "space" in the $\mathcal{L}$-representation of G_{out}.

Let us formalize the idea of "available space" mentioned in steps 5 and 6 in the above procedure. Let Γ be any $\mathcal{L}$-representation of some graph G and C be a 4-cycle in G. A *frame for* C is a 3-dimensional axis-aligned box F together with an injective mapping of $V(C)$ onto the facets of F such that the two facets without a preimage are adjacent. Every frame has one of two possible types. If two opposite vertices of C are mapped onto two opposite facets of F, then F has type $(\perp\!-\!||)$; otherwise, F has type $(\perp\!-\!\perp)$; see Fig. 12b. Finally, for an almost-optimal 1-planar graph G with corresponding quadrangulation Q and outer face C, and a given frame F for C, we say that an $\mathcal{L}$-representation Γ of G *fits into* F if replacing the boxes or $\mathcal{L}$'s for the vertices in C by the corresponding facets of F yields a proper contact representation of $G - E(G[C])$ that is strictly contained in F.

Before we prove this Section's main result, namely Theorem 3, we need one last lemma addressing

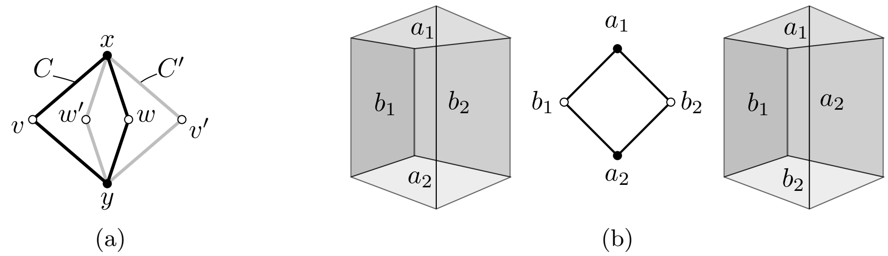

Figure 12: (a) Illustration for the proof of Lemma 10. (b) A frame of type $(\perp-||)$ (left) and of type $(\perp-\perp)$ (right).

the structure of maximal separating 4-cycles in almost-optimal 1-planar graphs.

Lemma 10. *Let G be an almost-optimal 1-planar graph with corresponding quadrangulation Q. Then all maximal separating 4-cycles of Q are interior-disjoint, unless two inner vertices w and w' of Q are adjacent to two outer vertices of Q.*

Proof. When two maximal separating 4-cycles C and C' are not interior-disjoint, then some vertex from C lies strictly inside C' and some vertex from C' lies strictly inside C. It follows that $V(C) \cap V(C')$ is a pair x, y of two vertices from the same bipartition class of Q, say $x, y \in B$, and that some $v \in V(C)$ lies strictly outside C' and some $v' \in V(C')$ lies strictly outside C. We have $v, v' \in W$ and that $C^* = (x, v, y, v')$ is a 4-cycle whose interior strictly contains C and C'. By the maximality of C and C' it follows that C^* is not separating. As the vertices $w \in V(C) \setminus V(C^*)$ and $w' \in V(C') \setminus V(C^*)$ lie strictly inside C^*, C^* must be the outer cycle of Q and w, w' are the desired vertices. □

Theorem 3. *Every optimal 1-planar graph $G = (V, E)$ has an $\mathcal{L}$-representation and it can be computed in $\mathcal{O}(|V|^2)$ time.*

Proof. Fix any 1-planar embedding of G and let Q be the corresponding quadrangulation with outer cycle C_{out}. Following algorithm **L-Contact**, we distinguish two cases. If (**Case 1**) some inner vertex w of Q has two neighbors on C_{out} we let $\mathcal{C}$ be the set of the two 4-cycles in Q that consist of w and 3 vertices of C_{out}. Otherwise (**Case 2**), let $\mathcal{C}$ be the set of all maximal separating 4-cycles in Q. By Lemma 10 the cycles in $\mathcal{C}$ are interior-disjoint. As in step 4 we define G_{out} to be the optimal 1-planar (multi)graph obtained from G by replacing for each $C \in \mathcal{C}$ all vertices strictly inside C by a pair of crossing edges. Note that in Case 1 the quadrangulation corresponding to G_{out} is $K_{2,3}$ with inner vertex w. We proceed by proving the following claim, which corresponds to step 5 in the algorithm.

Claim 1. *Let H be an almost-optimal 1-planar (multi)graph whose corresponding quadrangulation Q_H is either $K_{2,3}$ or has no separating 4-cycles. Let $\mathcal{C}$ be a set of facial 4-cycles of Q_H, different from C_o, and H' be the graph obtained from H by removing the crossing edges in each $C \in \mathcal{C}$. Then for any given frame F for the outer cycle C_o of Q_H one can compute an $\mathcal{L}$-representation Γ of H' fitting into F such that for every $C \in \mathcal{C}$ there is a frame $F_C \subseteq F$ for C that is interior-disjoint from all boxes and $\mathcal{L}$'s in Γ.*

Proof of Claim 1.

Case 1, $Q_H = K_{2,3}$. Let w be the inner vertex of H. Without loss of generality let $F = [0, 5] \times [0, 5] \times [0, 4]$ and let $V(C_o)$ be mapped onto the top, back left, bottom and back right facets of F. We define the $\mathcal{L}$ for w to be the union of $[0, 3] \times [2, 3] \times [0, 4]$ and $[2, 3] \times [0, 3] \times [0, 4]$. Further define four boxes $F_1 = [0, 2] \times [0, 1] \times [0, 1]$, $F_2 = [0, 2] \times [0, 1] \times [3, 4]$, $F_3 = [3, 4] \times [0, 1] \times [0, 4]$ and $F_4 = [0, 1] \times [3, 4] \times [0, 4]$, each completely contained in F and disjoint from the $\mathcal{L}$ for w; see Fig. 13. Each F_i is a frame for a 4-tuple containing w and exactly three vertices of C_o, $i = 1, 2, 3, 4$. Thus independent of the type of F and the neighbors of w in Q_H, we find a frame for both inner faces of Q_H.

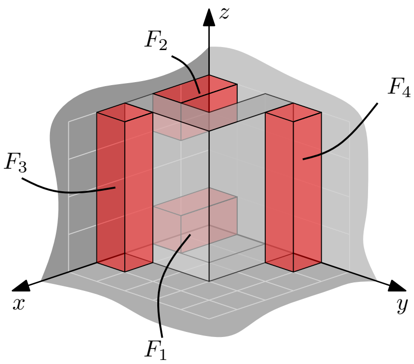

Figure 13: Construction for Case 1 in the proof of Claim 1.

Case 2, $Q_H \neq K_{2,3}$. Let B and W be the bipartition classes of Q_H and $C_o = (v_1, w_1, v_2, w_2)$ with $v_i \in B$ and $w_i \in W$, $i = 1, 2$. Without loss of generality v_1, v_2, w_1 are mapped onto the back left, back right and top facets of F, respectively, and w_2 is mapped onto the bottom facet if (**Case 2.1**) F has type $(\perp - ||)$ and onto the front left facet if (**Case 2.2**) F has type $(\perp - \perp)$. Let H^* be the graph obtained from H by inserting a pair of crossing edges in C_o, leaving v_1, w_2 and v_2 on the unbounded region. By assumption, H^* is a prime 1-planar graph and thus by Lemma 9 $H^*_B = H^*[B]$ and $H^*_W = H^*[W]$ are planar 3-connected and dual to each other. We choose v_3 to be the clockwise next vertex after v_2 on the outer face of H^*_B and compute (using Corollary 2) a shelled box-contact representation Γ^* of H^*, in which w_2 is represented as the bounding box $F^* = [0, n]^3$, $n \in \mathbb{N}$, and v_1, v_2, w_1 as $[0, n] \times [0, 1] \times [0, n]$, $[0, 1] \times [0, n] \times [1, n] \times [1, n] \times [n-1, n]$, i.e., these boxes constitute the back left, back right and top facets of F^*, respectively.

Next we show how to create a frame for each facial 4-cycle $C \in \mathcal{C}$. Let a_1, b_1, a_2, b_2 be the vertices of C in cyclic order. Assume without loss of generality that $a_1, a_2 \in W$ and $b_1, b_2 \in B$. Thus (a_1, a_2) and (b_1, b_2) are crossing edges of H^*_W and H^*_B, respectively. In the Schnyder wood of H^*_W underlying Corollary 2 exactly one of (a_1, a_2), (b_1, b_2) is uni-directed, say (a_1, a_2) is uni-directed in tree $\mathcal{T}_1$. Then there is a point in $\mathbb{R}^3$ in common with all four boxes in Γ^* corresponding to vertices of C. Moreover, by Lemma 7 boxes b_1, a_2, b_2 touch box a_1 with their y^+, z^+, y^- facets, respectively; see Fig. 14. Now we can increase the lower z-coordinate of the box a_1 by some $\varepsilon > 0$ so that a_1 and a_2 lose contact and between these two boxes a cubic frame F_C with side length ε is created; see again Fig. 14. Note that by Lemma 7 the z^- facet of a_1 makes contact only with a_2 and hence if ε is small enough all other contacts in Γ^* are maintained. We apply this operation to each $C \in \mathcal{C}$ and obtain a shelled box-representation Γ' of H'.

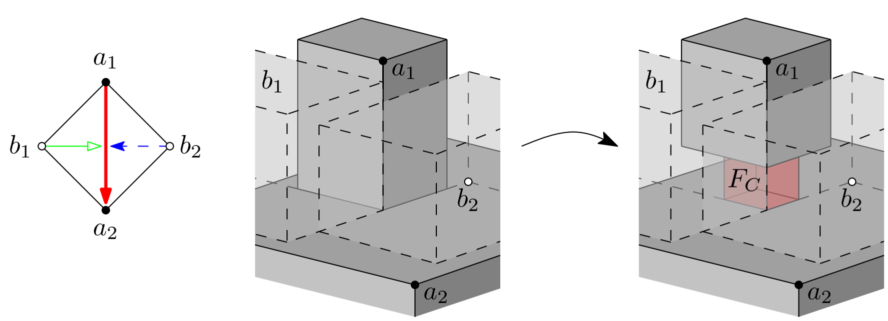

Figure 14: Creating a frame F_C for an inner facial cycle $C = (a_1, b_1, a_2, b_2)$ of Q_H by releasing the contact between a_1 and a_2.

Finally, we show how to modify Γ' to obtain an $\mathcal{L}$-representation of H' fitting the given frame F.

If (**Case 2.1**) F has type $(\perp-||)$, we define a new box for w_2 to be $[0, n+1] \times [0, n] \times [-1, 0]$. For each white neighbor of w_2 we union the corresponding box with another box that is contained in $[n, n+1] \times [0, n] \times [0, n]$ with bottom facet at $z = 0$ so that the result is an $\mathcal{L}$-shape. For each black neighbor of w_2 we set the lower z-coordinate of the corresponding box to 0; see Fig. 15. (This requires the proper contacts for outer edges of G_B, except for (v_1, v_2), to be parallel to the xz-plane, which we can easily guarantee.) We then apply an affine transformation mapping $[1, n+1] \times [1, n] \times [0, n-1]$ onto F. If (**Case 2.2**) F has type $(\perp-\perp)$, we define a new box for w_2 to be $[0, n] \times [n, n+1] \times [0, n]$ and apply an affine transformation mapping $[1, n] \times [1, n] \times [0, n-1]$ onto F. In both cases we have an $\mathcal{L}$-representation of H' fitting F. △

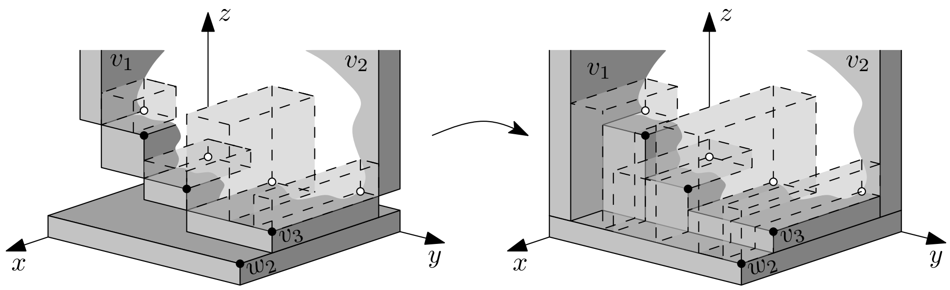

Figure 15: Modifying Γ' when F has type $(\perp-||)$ (Case 2.1) to find a representation fitting F.

By the claim above we can compute an $\mathcal{L}$-representation Γ_{out} of G_{out} fitting any given frame F_{out} for C_{out} in $\mathcal{O}(|V(G_{out})|)$ time. Moreover, Γ_{out} has a set of disjoint frames $\{F_C \mid C \in \mathcal{C}\}$. Following step 6 of algorithm **L-Contact**, for each $C \in \mathcal{C}$, let $G_{in}(C)$ be the almost-optimal 1-planar graph given by all vertices and edges of G on and strictly inside C. Recursively applying the claim we can compute an $\mathcal{L}$-representation Γ_C of $G_{in}(C)$ fitting the frame F_C for C in Γ_{out}. Clearly, $\Gamma = \Gamma_{out} \cup \bigcup_{C \in \mathcal{C}} \Gamma_C$ is an $\mathcal{L}$-representation of G fitting F_{out}. We pick a frame F_{out} of arbitrary type for C_{out} to complete the construction. □

5 Conclusion and Open Questions

In this paper we presented new results about primal-dual contact representations in 3D. In particular, we showed that a 3-connected planar graph and its dual has a box-contact representation and that an optimal 1-planar graph has an $\mathcal{L}$-contact representation. Many interesting problems remain open.

1. Representing graphs with contacts of constant-complexity 3D shapes, such as $\mathcal{L}$'s, is open for many graph classes with a linear number of edges, such as 1-planar graphs, quasi-planar graphs and other nearly planar graphs. In particular, does there exist an $\mathcal{L}$-contact representation of every 1-planar graph?

2. In 2D, a planar graph has a contact representation with rectangles if and only if it contains no separating triangle. Which graphs have 3D box-contact representations?

3. It is known that any planar graph admits a proper contact representation with boxes in 3D and a non-proper contact representation with cubes (boxes with equal sides). Does every planar graph admit a proper contact representation with cubes?

4. Given an orthogonal surface S corresponding to the Schnyder wood of a 3-connected plane graph, how can one extend S into a primal-dual box-contact representation using just topological properties of S?

Acknowledgments

We thank Michael Bekos, Therese Biedl, Franz Brandenburg, Michael Kaufmann, Giuseppe Liotta for useful discussions about different variants of these problems.

References

[1] E. Andreev. On convex polyhedra in lobachevskii spaces. *Mat. Sbor.*, 123(3):445–478, 1970.

[2] D. Avis and M. E. Houle. Computational aspects of Helly's theorem and its relatives. *International Journal of Computational Geometry and Applications*, 5(4):357–367, 1995.

[3] M. Badent, C. Binucci, E. D. Giacomo, W. Didimo, S. Felsner, F. Giordano, J. Kratochvíl, P. Palladino, M. Patrignani, and F. Trotta. Homothetic triangle contact representations of planar graphs. In *CCCG*, pages 233–236, 2007.

[4] M. Badent, U. Brandes, and S. Cornelsen. More canonical ordering. *Journal of Graph Algorithms and Applications*, 15(1):97–126, 2011.

[5] M. J. Bannister, W. E. Devanny, D. Eppstein, and M. T. Goodrich. The Galois complexity of graph drawing: Why numerical solutions are ubiquitous for force-directed, spectral, and circle packing drawings. In *Graph Drawing*, pages 149–161, 2014.

[6] O. Bernardi and E. Fusy. Schnyder decompositions for regular plane graphs and application to drawing. *Algorithmica*, 62(3–4):1159–1197, 2012.

[7] A. Bezdek. On the number of mutually touching cylinders. *Combinatorial and Computational Geometry*, 52:121–127, 2005.

[8] K. Bezdek and S. Reid. Contact graphs of unit sphere packings revisited. *Journal of Geometry*, 104(1):57–83, 2013.

[9] R. Bodendiek, H. Schumacher, and K. Wagner. Über 1-optimale graphen. *Mathematische Nachrichten*, 117(1):323–339, 1984.

[10] F. Brandenburg, D. Eppstein, A. Gleißner, M. Goodrich, K. Hanauer, and J. Reislhuber. On the density of maximal 1-planar graphs. In *Graph Drawing*, pages 327–338, 2013.

[11] D. Bremner, W. Evans, F. Frati, L. Heyer, S. Kobourov, W. Lenhart, G. Liotta, D. Rappaport, and S. Whitesides. Representing graphs by touching cuboids. In *Graph Drawing*, pages 187–198, 2012.

[12] G. Brinkmann, S. Greenberg, C. Greenhill, B. McKay, R. Thomas, and P. Wollan. Generation of simple quadrangulations of the sphere. *Discrete Math.*, 305(1–3):33–54, 2005.

[13] A. L. Buchsbaum, E. R. Gansner, C. M. Procopiuc, and S. Venkatasubramanian. Rectangular layouts and contact graphs. *ACM Transactions on Algorithms*, 4(1), 2008.

[14] S. Chaplick, S. G. Kobourov, and T. Ueckerdt. Equilateral L-contact graphs. In *Graph-Theoretic Concepts in Computer Science (WG)*, pages 139–151, 2013.

[15] C. R. Collins and K. Stephenson. A circle packing algorithm. *Computational Geometry: Theory and Applications*, 25(3):233–256, 2003.

[16] J. Czyzowicz, E. Kranakis, and J. Urrutia. A simple proof of the representation of bipartite planar graphs as the contact graphs of orthogonal straight line segments. *Information Processing Letters*, 66(3):125–126, 1998.

[17] H. de Fraysseix and P. O. de Mendez. On topological aspects of orientations. *Discrete Mathematics*, 229(1–3):57–72, 2001.

[18] H. de Fraysseix and P. O. de Mendez. Representations by contact and intersection of segments. *Algorithmica*, 47(4):453–463, 2007.

[19] H. de Fraysseix, P. O. de Mendez, and J. Pach. Representation of planar graphs by segments. *Intuitive Geometry*, 63:109–117, 1991.

[20] H. de Fraysseix, P. O. de Mendez, and P. Rosenstiehl. On triangle contact graphs. *Combinatorics, Probability and Computing*, 3:233–246, 1994.

[21] H. de Fraysseix, J. Pach, and R. Pollack. How to draw a planar graph on a grid. *Combinatorica*, 10(1):41–51, 1990.

[22] I. Fabrici and T. Madaras. The structure of 1-planar graphs. *Discrete Mathematics*, 307(7–8):854–865, 2007.

[23] S. Felsner and M. C. Francis. Contact representations of planar graphs with cubes. In *Symposium on Computational Geometry*, pages 315–320, 2011.

[24] S. Felsner and F. Zickfeld. Schnyder woods and orthogonal surfaces. *Discrete & Computational Geometry*, 40(1):103–126, 2008.

[25] E. R. Gansner, Y. Hu, and S. G. Kobourov. Visualizing graphs and clusters as maps. In *IEEE Computer Graphics and Applications*, pages 2259–2267, 2010.

[26] D. Gonçalves, B. Lévêque, and A. Pinlou. Triangle contact representations and duality. *Discrete & Computational Geometry*, 48(1):239–254, 2012.

[27] P. Hliněný. Classes and recognition of curve contact graphs. *Journal of Combinatorial Theory Series B*, 74(1):87–103, 1998.

[28] P. Hliněný and J. Kratochvíl. Representing graphs by disks and balls (a survey of recognition-complexity results). *Discrete Mathematics*, 229(1–3):101–124, 2001.

[29] D. House and C. Kocmoud. Continuous cartogram construction. In *Visualization*, pages 197–204, 1998.

[30] G. Kant. Drawing planar graphs using canonical ordering. *Algorithmica*, 16(1):4–32, 1996.

[31] S. G. Kobourov, T. Ueckerdt, and K. Verbeek. Combinatorial and geometric properties of planar Laman graphs. In *Symposium on Discrete Algorithms*, pages 1668–1678, 2013.

[32] P. Koebe. Kontaktprobleme der konformen Abbildung. *Berichte über die Verhandlungen der Sächsischen Akad. der Wissen. zu Leipzig. Math.-Phys. Klasse*, 88:141–164, 1936.

[33] J. Kratochvíl and J. Matousek. Intersection graphs of segments. *Journal of Combinatorial Theory Series B*, 62(2):289–315, 1994.

[34] J. Michalek, R. Choudhary, and P. Papalambros. Architectural layout design optimization. *Engineering Optimization*, 34(5):461–484, 2002.

[35] B. Mohar. Circle packings of maps in polynomial time. *European Journal of Combinatorics*, 18(7):785–805, 1997.

[36] J. Pach and G. Tóth. Graphs drawn with a few crossings per edge. *Combinatorica*, 17:427–439, 1997.

[37] E. Raisz. The rectangular statistical cartogram. *Geographical Review*, 24(2):292–296, 1934.

[38] G. Ringel. Ein sechsfarbenproblem auf der kugel. *Abhandlungen aus dem Mathematischen Seminar der Universitat Hamburg*, 29(1–2):107–117, 1965.

[39] P. Rosenstiehl and R. E. Tarjan. Rectilinear planar layouts and bipolar orientations of planar graphs. *Discrete & Computational Geometry*, 1(1):343–353, 1986.

[40] W. Schnyder. Embedding planar graphs on the grid. In *Symposium on Discrete Algorithms*, pages 138–148, 1990.

[41] H. Schumacher. Zur struktur 1-planarer graphen. *Math. Nachrichten*, 125:291–300, 1986.

[42] B. Shneiderman. Tree visualization with tree-maps: A 2-D space-filling approach. *ACM Transactions on Graphics*, 11(1):92–99, 1992.

[43] Y. Suzuki. Re-embeddings of maximum 1-planar graphs. *SIAM Journal on Discrete Mathematics*, 24(4):1527–1540, 2010.

[44] C. Thomassen. Interval representations of planar graphs. *Journal of Combinatorial Theory Series B*, 40(1):9–20, 1988.

[45] W. Tobler. Thirty five years of computer cartograms. *Annals of the Association of American Geographers*, 94:58–73, 2004.

[46] J. D. Ullman. *Computational Aspects of VLSI.* Computer Science Press, 1984.